energies

MDPI

Article

An Improved Over-Speed Deloading Control of Wind Power Systems for Primary Frequency Regulation Considering Turbulence Characteristics

Xiaolian Zhang [1,*], Baocong Lin [2], Ke Xu [1], Yangfei Zhang [1], Sipeng Hao [1] and Qi Hu [1]

[1] School of Electric Power Engineering, Nanjing Institute of Technology, Nanjing 211167, China
[2] School of Automation, Nanjing University of Science and Technology, Nanjing 210094, China
* Correspondence: zhangxl530@163.com

Abstract: Wind power systems participating in primary frequency regulation have become a novel trend. In order to solve the problem of the over-speed deloading (OSD) control of wind power systems failing to provide reserved capacity for primary frequency regulation while under turbulent winds, this paper analyzes the influence mechanism of turbulence characteristics on the OSD control and the relationship between the reserve capacity of OSD control and the deloading power coefficient under turbulent wind speeds, while also quantifying the relationship between the turbulence characteristic index and deloading power coefficient. The range of the deloading power coefficient is obtained accordingly, based on which improved OSD control is proposed to dynamically optimize the deloading power coefficient according to the turbulence characteristics, which improves the frequency regulation performance of wind power systems under turbulent wind speed. According to the simulations and experimental results, the improved method proposed in this paper has good effectiveness and superiority in frequency regulation effect and rotor speed performance.

Keywords: wind power system; primary frequency regulation; OSD control; turbulence characteristics

Citation: Zhang, X.; Lin, B.; Xu, K.; Zhang, Y.; Hao, S.; Hu, Q. An Improved Over-Speed Deloading Control of Wind Power Systems for Primary Frequency Regulation Considering Turbulence Characteristics. *Energies* **2023**, *16*, 2813. https://doi.org/10.3390/en16062813

Academic Editors: Francesco Castellani and Abu-Siada Ahmed

Received: 4 January 2023
Revised: 7 March 2023
Accepted: 15 March 2023
Published: 17 March 2023

1. Introduction

With the proposal of "carbon peak" and "carbon neutrality", renewable energy sources such as wind and solar energy have been vigorously developed in China, but the high proportion of wind power results in some brand-new problems. Nowadays, mainstream wind turbines use converters to connect to the power grid, causing the uncoupled relationship between the rotor speed of wind turbines and the power grid's frequency, which leads to decreased inertia of the power grid with a high wind power penetration rate, reducing the frequency stability of the system [1]. Therefore, some research about frequency regulation by wind power systems has been carried out.

At present, the methods of wind power systems participating in frequency regulation can be divided into rotor kinetic energy control, power reserve control and wind power-energy storage hybrid control [1,2]. The rotor kinetic energy control, such as the droop control and inertia control, can maintain the frequency adjustment for a short time but will eventually lead to a second drop in the system frequency [3,4]. The power reserve control, such as the over-speed deloading (OSD) control and variable pitch control, can preset reverse capacity by part-load operation. The wind power-energy storage hybrid control can provide enough power for system frequency adjustment by the energy storage system, but this type of control needs to add storage units which increases the cost of construction and maintenance [5,6]. The comparison of these methods is shown in Table 1.

Table 1. The comparison of different control methods.

The Control Methods		Work Principle	Advantage	Disadvantage
Rotor kinetic energy control	Droop control	Using the kinetic energy of wind turbine rotor	Simple, easy to carry out	Leading to a second drop in system frequency
	Inertia control	Using the kinetic energy of wind turbine rotor	Simple, easy to carry out	Leading to a second drop in system frequency
Power reserve control	The over-speed deloading control	Presetting reverse capacity by part-load operation	Easy to control, can provide more power	Reducing the wind power efficiency
	Variable pitch control	Presetting reverse capacity by part-load operation	Can provide more power	Reducing the wind power efficiency
Wind power-energy storage hybrid control	Cooperative control	Power support by both systems	Better performance than other methods	More complex and more expensive

The OSD control has the advantages of not needing to add equipment and being easy to control [7,8], so it is widely applied in wind power systems. References [9–11] apply OSD control to a single wind power system and wind farm, improving the performance of the wind power system participating in power grid frequency regulation to a certain extent. However, the research above is all conducted under constant wind speed, and whether the same results would be obtained under turbulence wind speed needs further study.

Although some control methods consider the change in wind speed, it is mainly a rough classification of wind speed conditions. For example, wind speed is divided into three levels and control parameters are set separately according to these levels. It has also been studied that the wind speed is divided into three levels, and the pitch control and OSD control are used to coordinate at different levels to achieve frequency regulation [9,10]. The reference [12] considered the impact of wind power and load power fluctuations on system frequency and smoothed the output power of wind turbines to improve frequency stability. However, these studies are relatively rough when considering wind speed characteristics, ignoring the turbulence characteristics, such as average wind speed and turbulence intensity.

The actual wind speed is mainly turbulent wind speed with strong randomness and fluctuations, which will lead to difficulties or failures in wind power control [13,14]. Additionally, fluctuating wind power under turbulent wind speed will also cause system frequency changes [15,16]; therefore, it is necessary to study the influence of turbulent wind speed on the frequency regulation performance of wind power and improve the control effect under turbulent wind speed.

All in all, the existing control strategies mainly focus on constant wind speed, but the dynamic response of wind power systems under turbulent wind speed is different from that of constant wind speed [13,14], which weakens the effect of the traditional control strategy. In addition, different turbulence characteristics also have different influences on the control effect, and the existing research has not studied these issues.

In the previous research, the author analyzed the influence of turbulence characteristics on system frequency and proposed an improved frequency controller [17], but this method requires additional power control blocks. Additionally, through further research, it was

found that the OSD control could not provide preset reserve capacity under turbulent wind speed, which weakened its frequency regulation ability under turbulent wind speed.

Therefore, further study has been conducted based on the author's previous research in this paper to obtain an improved OSD control. The main contributions of this paper are as follows:

1. the influence mechanism of turbulent wind speed on the OSD control is analyzed;
2. the relationship between the reserve capacity of OSD control and deloading power coefficient under turbulent wind speed is analyzed, and the quantitative relationship between the turbulence characteristics and the deloading power coefficient is obtained;
3. based on the relationships above, the range of the deloading power coefficient of the OSD control is obtained, and a reasonable algorithm for setting the coefficient is designed, therefore the OSD control is improved to respond to turbulence characteristics.

Through simulations and experiments based on the experimental platform, it is verified that the improved strategy can effectively reserve enough power for frequency regulation. Compared with existing methods, the improved strategy has a better frequency regulation effect and rotor speed performance.

2. The Model and Control Strategy

2.1. The Model of Wind Power Participating in Primary Frequency Regulation

The wind power system is a combination of mechanical, electrical and control equipment, converting wind energy into electric power [18]; it usually consists of wind turbines, a transmission system, a variable pitch system, an electrical system and a control system. In this paper, according to [19], a model for wind power systems participating in primary frequency regulation of the power grid is established, including wind turbine models, maximum power point tracking (MPPT) controllers, frequency controllers, and transmission systems, as shown in Figure 1.

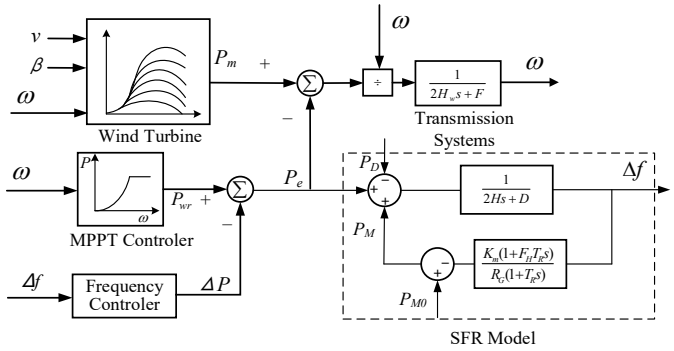

Figure 1. The model of wind power participating in primary frequency regulation of power grid.

According to Bertz's Law, the mechanical power of wind turbine captured from wind energy P_m is:

$$\begin{cases} P_m = 0.5\rho\pi R^2 v^3 C_p(\lambda,\beta) \\ C_p = 0.5(116/\lambda - 0.4\beta - 5)e^{-21/\lambda_1} + 0.0068\lambda \\ \lambda_1 = [1/(\lambda + 0.08\beta) - 0.035/(\beta^3+1)]^{-1} \end{cases} \quad (1)$$

where ρ is the air density; R is the radius of the wind turbine; v is the wind speed; C_p is the power coefficient, β is the pitch angle, λ is the tip speed ratio, it is defined as $\lambda = \omega R/v$, ω is rotor speed for wind turbines.

The mechanical power absorbed by the wind turbine is transferred to the generator through the transmission system. Here, the transmission system model is shown as follows:

$$\omega = \frac{1}{2H_w s + F}(T_m - T_e) \quad (2)$$

where H_w is the inertia coefficient of the transmission system, and F is the friction coefficient of the transmission system. The detail of Equation (2) can be seen in [19].

The MPPT control of the wind turbines uses the power curve feedback method, the active power reference $P_{\max}$ can be defined by the equation below [20].

$$\begin{cases} P_{\max} = K_{opt}\omega^3 \\ K_{opt} = \dfrac{0.5\rho\pi R^5 C_p^{\max}}{\lambda_{opt}^3} \end{cases} \tag{3}$$

The power grid is modeled by a low-order system frequency response (SFR) model shown in Figure 1. This model can be used to estimate the frequency changes under power disturbance [18]. In Figure 1, P_e is the output power of the wind turbine; P_M is a traditional synchronous generator output power, P_{M0} is the initial value, P_D is load power, Δf is power grid frequency deviation, H is inertia constant, D is damping factor, K_m is power gain factor of the synchronous generator, F_H is the fraction of total power generated by the high-pressure turbine, T_R is reheat time constant, R_G is the adjustment factor of the synchronous generator.

2.2. OSD Control

When the wind turbine operates at the maximum power point, there is no reserve capacity for frequency regulation, but when the wind turbine operates at a point with a larger rotor speed, the output power of the wind turbine can be reduced, and the reserve capacity can be obtained, as the P_{del} shown in Figure 2. This method is called the over-speed deloading (OSD) control. The OSD control is generally adopted to realize the power reduction operation of the wind turbine [2].

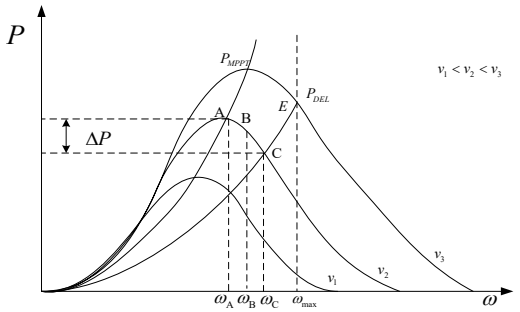

Figure 2. Working principle of OSD control.

The OSD control tracks deloading power curve P_{del}; the relationship between P_{del} and rotor speed ω can be expressed as follows:

$$\begin{cases} P_{del} = K_d K_{opt}\omega^3 \\ K_d = 1 - d\% \end{cases} \tag{4}$$

where K_d is the deloading power coefficient, and $d\%$ is the deloading coefficient.

The working principle of OSD control is shown in Figure 2. The MPPT curve shifts to the right, from the optimal working point A to the suboptimal working point C, at which time the wind power output decreases, reserving certain power. When the system frequency decreases, the rotor speed decreases from ω_C to ω_B, the MPPT curve shifts to the left, and the working point shifts from point C to point B so that the wind turbine output increases in response to the system frequency change.

3. Analysis of Difficulties and Mechanism of OSD Control under Turbulent Wind Speed

Wind is caused by atmospheric movement. Due to the complex surface topography and the change in air temperature, pressure, or humidity, the atmosphere's movement is

a random and turbulent motion, which makes the wind speed fluctuate constantly, and these are the causes of turbulence. Therefore, these factors will influence the values of wind speed v, as well as the air density ρ; the wind power P_m will also be influenced according to Equation (1). It can be seen that wind speed fluctuates constantly, this is one cause of frequency deviation; therefore, wind speed fluctuation should be addressed to guarantee the stable operation of the system.

Under constant wind speed, when the OSD control is used, the wind turbine can work stably at the deloading operating point and provide the reserve capacity stably. While under turbulent wind speed, due to the fluctuation of wind speed and the influence of moment of inertia, the wind turbine cannot work at the deloading operating point in time and provide stable reserve capacity. In addition, it will even reduce the reserve capacity and weaken the frequency regulation effect. Therefore, the control strategies based on constant wind speed or steady-state will have new problems.

The example shown in Figure 3 shows that the system response of turbulent wind speed is different from that of constant wind speed with the same control parameters, the difference in dynamic performance and the influence of wind turbulence on the control are also verified.

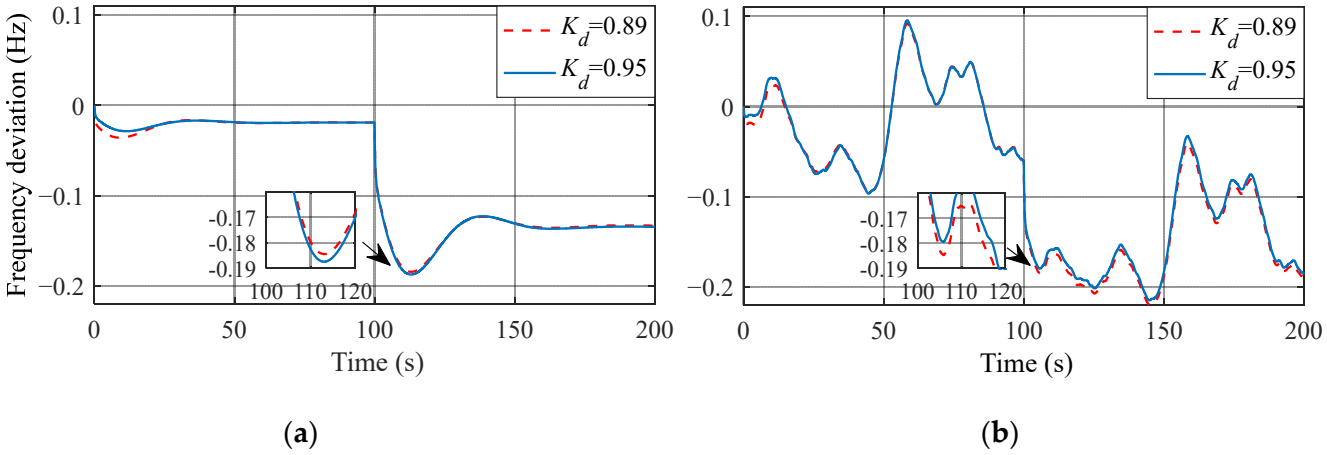

Figure 3. Frequency regulation effect of OSD control at different wind conditions. (**a**) Constant wind speed, (**b**) turbulent wind speed.

It is found that the slope of the optimal power curve is reduced when the wind turbine uses OSD control (such as P_{del} shown in Figure 2). Therefore, the difference between mechanical torque and electromagnetic torque is increased, which improves the performance of the wind power system in tracking the maximum power point under turbulent wind speed [12], then the available reserve capacity will be reduced due to the improved wind energy capture efficiency. That means K_d will change the dynamic performance of the wind power system, and then affect the reserve capacity and frequency regulation effect of the wind power system. The elaboration is shown as follows.

Under constant wind speed, when the load suddenly increases at 100 s, the smaller the K_d is, the better the lowest frequency and then the better the frequency regulation effect will be, as shown in Figure 3a. However, under turbulent wind speed, the result is just the opposite. The smaller the K_d is, the more severe the frequency falls, as shown in Figure 3b.

Figure 4 shows the wind power output of the example shown in Figure 3b. It can be seen that when load suddenly increases at 100s, the wind power with K_d of 0.89 is lower than that of 0.95 and the MPPT control.

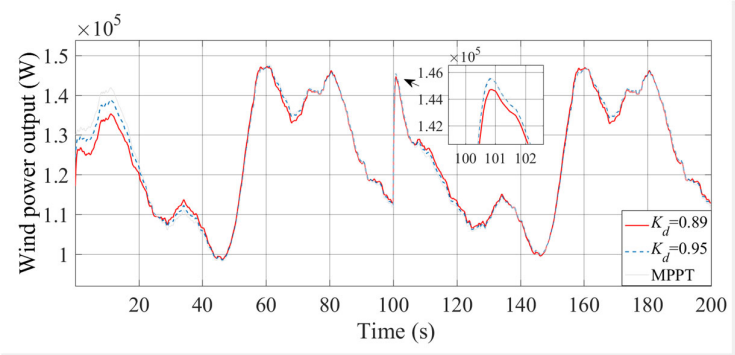

Figure 4. Wind power output under turbulent wind speed.

Table 2 shows the average wind energy capture efficiency, the average frequency deviation and the reserve capacity factor [21] under different strategies in Figure 4. The average wind energy capture efficiency is defined by Equation (5), and the average frequency deviation is defined by Equation (6).

Table 2. The average wind energy capture efficiency and reserve capacity factor under different strategies.

	K_d = 0.89	K_d = 0.95	MPPT
The average wind energy capture efficiency	0.4577	0.4575	0.4570
Reserve capacity factor k_{res}	1.03351	1.03353	1.03419
Average frequency deviation (Hz)	0.09732	0.09596	0.09576

The reserve capacity factor represents the reserve capacity of wind turbines. The higher the value, the lager the reserve capacity. The definition can be given by Equation (7) of Section 4.

$$C_{pavg} = \frac{\sum_{i=1}^{n} C_{pi}}{n} \tag{5}$$

where C_{pi} is the power coefficient of the ith sample, n is the total number of samples.

$$|\Delta f|_{avg} = \frac{\sum_{i=1}^{n} |\Delta f_i|}{n} \tag{6}$$

where Δf_i is the frequency deviation of the ith sample, n is the total number of samples, and the sampling period is 0.04 s.

It can be known from Table 2 that when K_d is 0.89, the wind energy capture efficiency is the highest, but the reserve capacity factor is the smallest, so it is difficult to provide enough power to support frequency adjustment in case of load fluctuation. The wind energy capture efficiency of MPPT control is the lowest, while the reserve capacity factor is the highest. It is verified that under turbulent wind speed, it will have a worse control effect with the same K_d as the constant wind speed.

So, the OSD control under turbulent wind speed does not play its function of reserving power for frequency regulation, and the frequency regulation effect is even worse than that of MPPT control without reserving power, which is the difficulty of OSD control applied to turbulent wind speed.

4. Improved OSD Control Considering Turbulence Characteristics

To solve the difficulties above, the influence of K_d on frequency regulation and the variation law of K_d under different turbulence characteristics are first analyzed, then an improved OSD control strategy for turbulent wind speed is proposed.

4.1. Analysis of the Influence of K_d on Frequency Regulation

4.1.1. Relationship between K_d and Frequency Deviation under Turbulent Wind Speed

In this paper, a typical turbulent wind speed with turbulence intensity level A in IEC-614000-1 standard is used, and the average frequency deviation of the power grid corresponding to different K_d is obtained through simulation.

The variation range of K_d is from 0.75 to 1.25, the statistical results are shown in Figure 5. It can be seen from Figure 5 that under turbulent wind speed, a different K_d will have different frequency control effects, and there is a K_d to maximize the average frequency deviation.

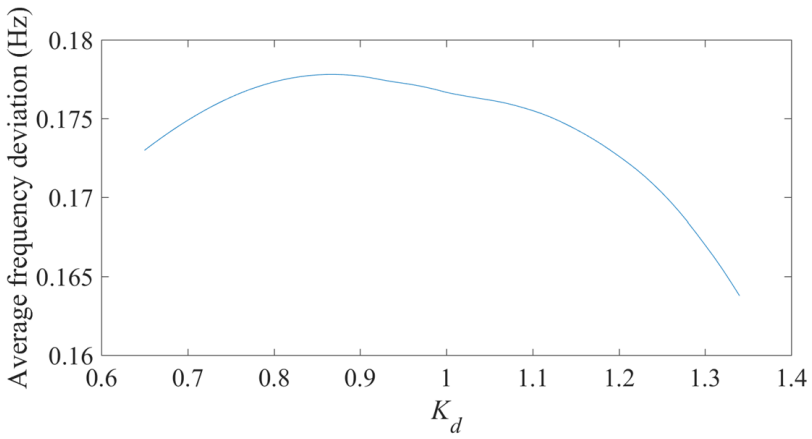

Figure 5. Relationship between average frequency deviation and K_d.

It is found that the K_d with the maximum average frequency deviation improves the tracking performance of the wind turbine, and maximizes its wind energy capture efficiency, thereby reducing the reserve capacity of the wind turbine, leading to the maximum average frequency deviation.

In this paper, the relationship between reserve capacity and K_d is further analyzed quantitatively. Here, the reserve capacity factor in reference [21] is used to define the reserve capacity of the wind turbine, as shown in Equation (7):

$$k_{\text{res}} = \frac{P_{wn} - P_w}{P_{wn} - P_{w1}} \tag{7}$$

where, P_{wn} is the rated power of the wind power system; P_w is the current wind power output; P_{w1} is the wind power at the lowest rotor speed.

To evaluate the reserve capacity at the same turbulent wind speed as the example shown in Figure 5, this paper calculates the average reserve capacity factor corresponding to different K_d, and the results are shown in Figure 6. It can be seen that the trend of average reserve capacity factor is opposite to the average frequency deviation shown in Figure 5, and there is a K_d to minimize the reserve capacity. The K_d is defined as K_{d_minres}. The result in Figure 6 verifies the influence mechanism mentioned in Section 3.

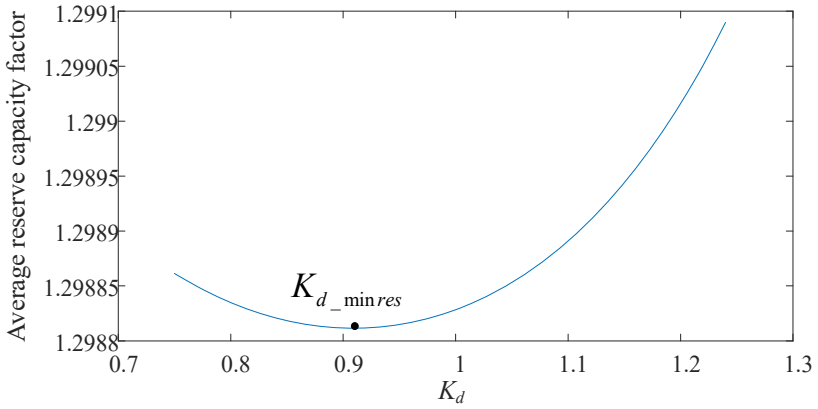

Figure 6. Relationship between average reserve capacity factor and K_d.

4.1.2. Mathematical Relationship between K_{d_minres} and Turbulence Characteristics

There is a K_{d_minres} to minimize the reserve capacity, and it is found that K_{d_minres} will change under different wind conditions; therefore, to analyze the relationship between K_{d_minres} and turbulence characteristics, a large number of wind speed samples are produced according to the given turbulence characteristic index, and then the traversal algorithm is used to obtain the K_{d_minres} of different turbulence characteristic indexes, then the change rule of K_{d_minres} under various turbulence characteristics can be achieved.

The average wind speed and turbulence intensity are selected as the turbulence characteristic indexes, the average wind speed ranges from 6.2 to 8.2 m/s with an interval of 0.2 m/s. According to the A, B and C three turbulence levels corresponding to IEC-614000-1 standard [22], the turbulence intensity value range is 0.18~0.32, and the interval is 0.02. Based on this, 70 wind speed samples with 10 kinds of average wind speeds and seven kinds of turbulence intensities can be obtained.

In each wind speed sample, the reserve capacity of the wind turbine is analyzed when the value of K_d is from 0.6 to 1.4, and the minimum reserve capacity of K_{d_minres} under each wind speed is achieved; the statistical results are shown in Figure 7.

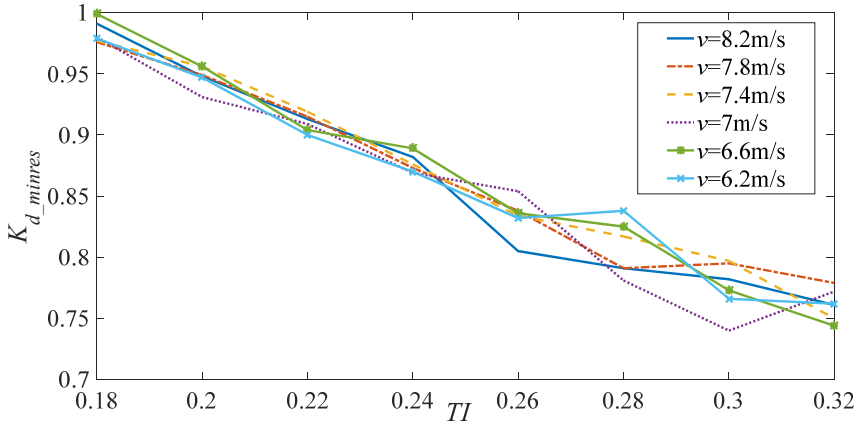

Figure 7. Relationship between K_{d_minres} and turbulence characteristic index.

It can be seen from Figure 7 that the K_{d_minres}-TI curves of different average wind speeds are relatively concentrated, when the average wind speed is constant, K_{d_minres} decreases with the increase of TI, and the change amplitude is obvious. Therefore, the impact of average wind speed to the K_{d_minres} is ignored, focusing on the relationship between K_{d_minres} and turbulence intensity TI. We obtained the average K_{d_minres}-TI curve,

then used the ordinary least squares method to fit the K_{d_minres}-TI curve. The fitting expression is as follows.

$$K_{d\_minres} = -1.6452 \cdot TI + 1.2718 \tag{8}$$

It can be seen from Figure 6 that, when K_d is set as K_{d_minres}, the average reserve capacity of the wind turbine is the lowest, and it is not good for frequency regulation. To make the OSD control effective, the selection of K_d need to avoid K_{d_minres}.

If K_d is greater than K_{d_minres}, in order to obtain more reserve capacity than MPPT control, K_d should be greater than one, and if it is changed to under-speed deloading control, in this case, deceleration will occur, taking the wind power system out of service. A large number of studies show that when using under-speed deloading control, the rotor speed will be at a low level, then stalling and taking the wind power system out of service are likely to occur [2]. Thus, the reasonable K_d should be less than K_{d_minres}.

4.1.3. The Range of K_d

According to the above analysis K_d should be less than K_{d_minres}. However, the smaller K_d is, the higher the rotor speed will be; there is an upper limit for the rotor speed of the wind turbine. When K_d is too small, the rotor speed will approach the upper limit, then MPPT control cannot be realized normally and it may easily cause damage to the rotor.

According to the deloading operation curve shown in Figure 2, point E is the upper limit of the rotor speed. At point E, the K_d and wind speed v will satisfy the following relationship.

$$K_d \cdot K_{opt} \cdot \omega_{\max}^3 = 0.5\rho\pi R^2 v^3 C_p(\omega_{\max} R/v, \beta) \tag{9}$$

while

$$K_d = \frac{0.5\rho\pi R^2 v^3 C_p(\omega_{\max} R/v, \beta)}{K_{opt} \cdot \omega_{\max}^3} \tag{10}$$

The relationship is shown in Figure 8. Because the equation is too complex, in order to simplify the control strategy, this paper uses the ordinary least square method to fit the curve, and the fitting expression is shown in Equation (11).

$$K_{d\min} = 0.1116 \cdot v - 0.6355 \tag{11}$$

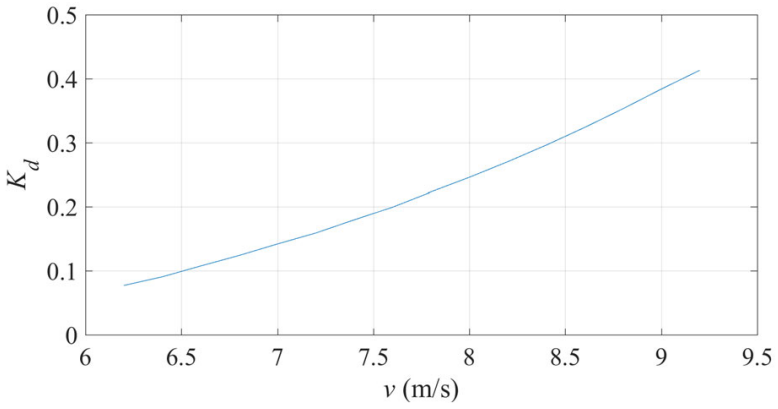

Figure 8. K_d-v curve when the rotor speed reaches the upper limit.

Therefore, in order to make sure the rotor speed does not exceed the limit and the OSD control can be normally used, the value of K_d should be greater than K_{dmin}.

In conclusion, to make the OSD control operate effectively under turbulent wind speed, K_d should be set in the range of $K_{dmin} < K_d < K_{d\_minres}$.

4.2. Improved OSD Control Considering Turbulence Characteristics

The above analysis gives a reasonable range of K_d. When K_d is set to K_{d_minres}, the wind turbine will provide the minimum reserve capacity and cannot provide enough power for frequency regulation; when K_d is set to K_{dmin}, the wind turbine will basically operate at the upper limit rotor speed, losing MPPT ability and greatly reducing the wind energy capture efficiency. Therefore, it is reasonable to set K_d as the midpoint of the range, which is shown in Equation (12):

$$K_d = \frac{K_{d\min} + K_{d\_minres}}{2} = 0.058 \cdot \overline{v} - 0.8226 \cdot TI + 0.31815 \quad (12)$$

where the average wind speed $\overline{v}$ is used to characterize the turbulent wind speed.

In this paper, Equation (12) is used to periodically adjust the K_d. The control block diagram is shown in Figure 9.

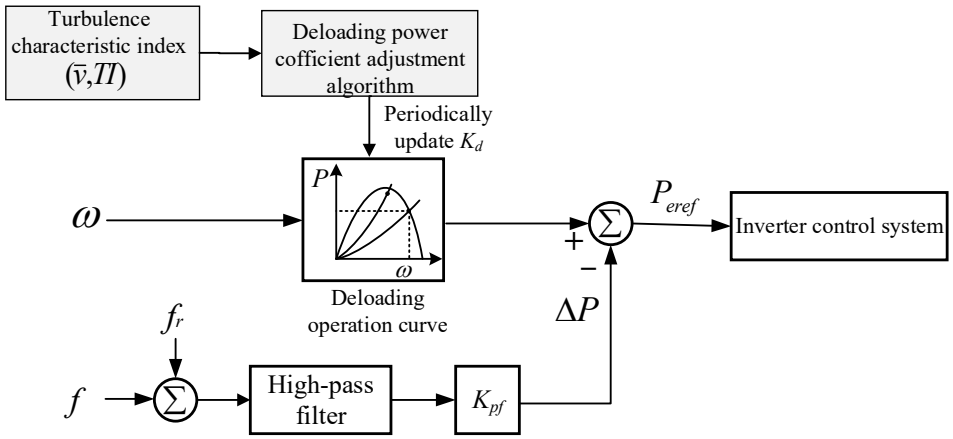

Figure 9. Block diagram of the improved OSD control.

The updating steps of K_d are as follows:

Step 1: initialize. Set the update cycle T of the deloading power coefficient, then put the number k of cycles into 0;

Step 2: let $k = k + 1$, and use the wind speed prediction to obtain the average wind speed $\overline{v}(k)$ and turbulence intensity $TI(k)$ of the wind speed during current cycle;

Step 3: calculate the $K_d(k)$ of the current cycle with Equation (12);

Step 4: judge whether the current cycle is over. If it is over, return to step 2.

5. Example Analysis

5.1. Simulation Analysis

In order to verify the superiority and effectiveness of the improved strategy in this paper, the method with fixed K_d (K_d is 0.9), the variable deloading power coefficient method proposed in [23] (hereafter referred to as variable K_d) and the improved strategy in this paper are compared.

1. Simulation parameters

A turbulent wind speed with average wind speed of 8 m/s and turbulence intensity of level A is used for simulation, and the load suddenly increases at 100 s.

The simulation parameters are shown in Table 3. The rated power of the wind power system in the simulation is 0.6 MW, and the rated wind speed is 12 m/s. The wind speed used in this paper mainly runs between 5 m/s and 12 m/s. The wind speed profile used in simulation is shown in Figure 10.

Table 3. Simulation parameters.

Wind turbine	R/m	20
	H_w/s	5.54
	λ_{opt}	5.8
	$C_p^{\max}$	0.4603
The Grid	H/s	4
	D	1
	K_m	0.95
	F_H	0.3
	T_R/s	8.0
	R_G	0.05
Controller	K_{pf}	2×10^5

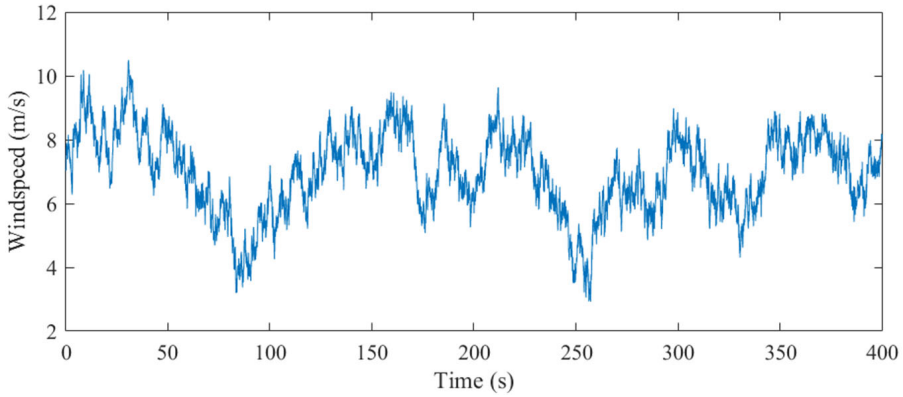

Figure 10. The wind speed used in simulation.

2. Analysis of simulation results

Figures 11–15, respectively, show the frequency deviation of the grid, wind power output, the operation curve of wind turbine before and after load change (95 s–120 s), and the K_d of different strategies.

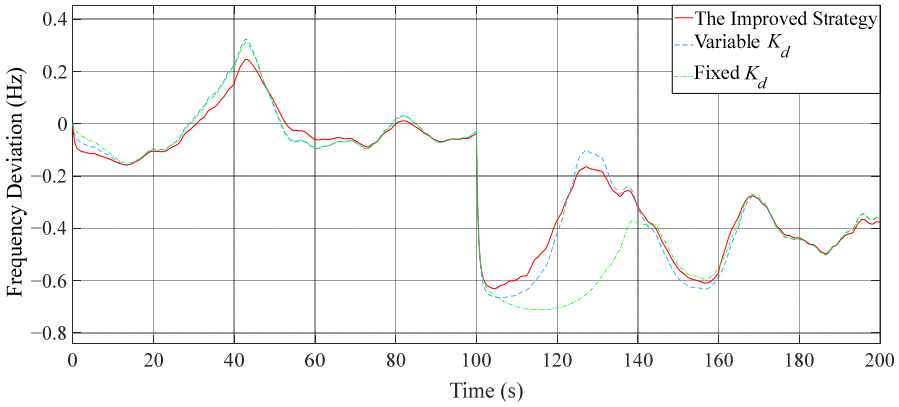

Figure 11. Frequency deviation.

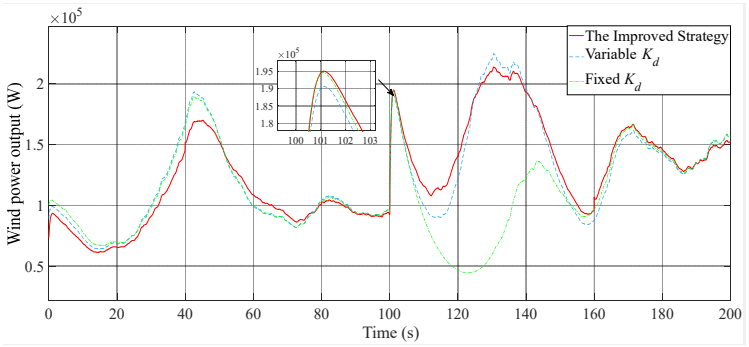

Figure 12. Wind power output.

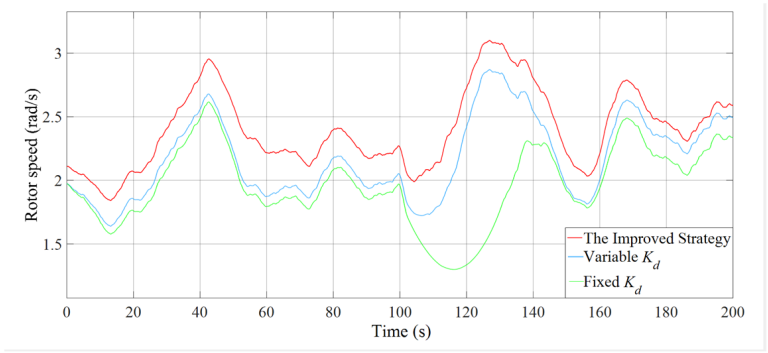

Figure 13. Rotor speed.

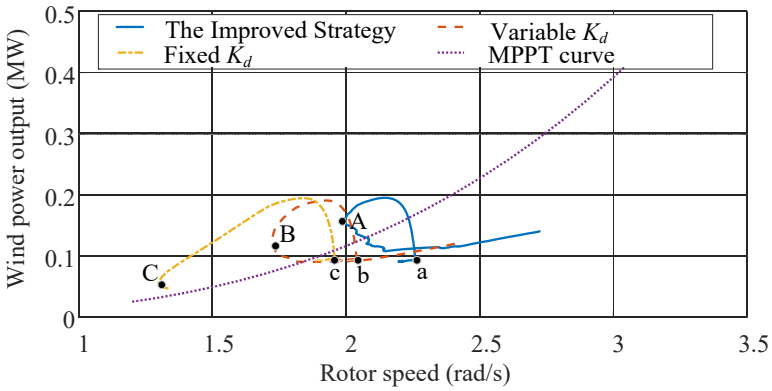

Figure 14. The operation curve before and after load fluctuation.

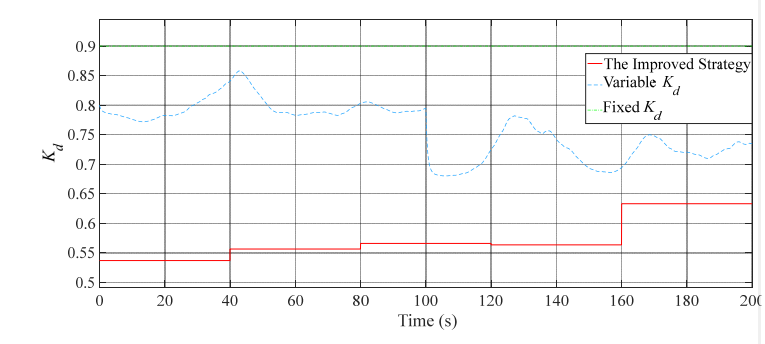

Figure 15. K_d of different methods.

It can be seen from Figure 11 that after sudden load increasing at 100 s, the frequency of the three strategies decreases, but the decline of the improved strategy in this paper is

significantly less than the other two strategies. And when the frequency support using the reserve capacity is completed, the improved strategy in this paper can recover the tracking of wind speed more quickly. However, the method with variable K_d and the one with fixed K_d have a longer recovery process due to the large drop in rotor speed. It can also be seen from Figure 12 that the improved strategy in this paper provides greater output power when the load suddenly increases at 100 s.

It can be seen from Figure 14 that a, b and c are the operating points of the three strategies at 100 s, A, B and C are the times when the rotor speed stops falling and begins to recover. When the load suddenly increases at 100 s, the operating points of the three strategies rise rapidly. After a short period of power support, the speed starts to drop, and the operating point moves to the left. It can be seen that the rotor speed drop of the improved strategy in this paper is obviously smaller than that of the other two strategies, and it can recover faster. However, the rotor speed of the fixed K_d method has a long time drop, which leads to continuous low output power that is not conducive to the frequency adjustment of the system. At the same time, the rotor stall problem is prone to occur, and there is a risk of making the wind power system go out of service.

Table 4 shows the average frequency deviation of the three strategies and the improvement of the improved strategy compared with other strategies.

Table 4. Average frequency deviation of different strategies.

	The Improved Strategy	**Variable K_d**	**Fixed K_d**
Average frequency deviation (Hz)	0.2510	0.2625	0.2994
Improvement of the improved strategy	——	4.58%	19.28%

The average wind energy capture efficiency of the three strategies is compared in Table 5.

Table 5. Average wind energy capture efficiency of different strategies.

	The Improved Strategy	**Variable K_d**	**Fixed K_d**
Average wind energy capture efficiency	0.4321	0.4389	0.4084

The wind energy capture efficiency of the improved strategy is higher than that of the method with fixed K_d and lower than that of variable K_d. When the load fluctuation occurs in the control with fixed K_d, the participation of the wind power system in frequency regulation leads to a serious drop in the rotor speed, so the wind energy capture efficiency is low. However, the rotor speed of the improved strategy in this paper is at a high level, so there is no serious rotor speed drop.

Due to the lower K_d than that of variable K_d, the wind energy capture efficiency of the improved strategy in this paper is lower than that of variable K_d, but the improved strategy obtains a better frequency regulation effect.

Wind energy capture efficiency and frequency regulation are always in conflict because the wind power system will give up tracking the maximum power point when it is participating in frequency regulation. The performance of frequency regulation becomes a more important goal. In the standard of GB/T 19963-2011 "Technical Regulations for Wind Farm Access to Power System", it is required that wind power systems should provide power to support the power system frequency. Additionally, the proportion of wind power systems in the power system will be larger and larger and the traditional synchronous generator will reduce, so wind power systems will play an important role in frequency regulation. In this case, the improved strategy is reasonable and valuable.

From the above analysis, it can be seen that the improved strategy in this paper can provide better reserve capacity, and the frequency regulation effect is much better. Compared with the control with fixed K_d, the frequency deviation can be increased by 19.28%, and the rotor speed can be well maintained to avoid the secondary frequency drop caused by rotor stall and rotor speed drop.

5.2. Experimental Analysis

In order to verify the effectiveness of the improved strategy, it is verified on the frequency regulation experimental platform with a wind power system. As shown in Figure 16, the experimental platform consists of seven parts: a synchronous generator simulator, wind turbine simulator, rectifier inverter for wind turbine simulator, synchronous drive inverters, synchronous machine dragging frequency converter, convergence cabinet and feed-back load. The experimental platform can simulate the frequency response of the power grid with wind turbines.

(a) Rectifier inverter for wind turbine simulator

(b) Feed-back load and synchronous drive inverters

(c) Convergence cabinet and synchronous machine dragging frequency converter

(d) Synchronous generator simulator

(e) Wind turbine simulator

Figure 16. Experimental platform.

Table 6 gives the main parameters of the experimental platform. Through the power scaling and inertia compensation algorithm [24], the wind turbine simulator in the experimental platform realizes the dynamic characteristics of the large capacity, large inertia wind power system, the frequency response characteristics of the actual power grid on the small capacity and low inertia experimental platform, which can be used to verify the control performance of the primary frequency regulation control strategy of the wind turbine. The wind turbine parameters simulated by the wind turbine simulator are the same as those of the simulation model.

A turbulent wind sequence with an average wind speed of 8 m/s and turbulence intensity level A is adopted for experimental analysis which is shown in Figure 17, and the load is set as in Figure 18. The improved strategy and the traditional deloading control with fixed K_d (K_d is 0.9) are compared by the experiment. The experimental results are shown in Figures 19–21.

Table 6. The main parameters of the experimental platform.

Parameters	The Value
Rated power of the wind turbine simulator	15 kW
Starting generation speed of the wind turbine simulator	0.48 rad/s
Rated power of the synchronous generator	25 kW
Inertia time constants of the synchronous generator	5.96 s
Rated speed of the synchronous generator	1800 r/min
Droop coefficient of the synchronous generator	0.05
The rated frequency of the grid	60 Hz
Rated power of feed-back loads	37 kVA
Control cycle of PLC	40 ms

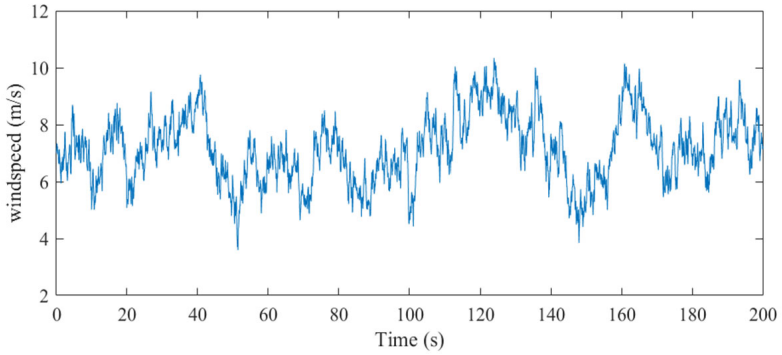

Figure 17. The wind speed used in experimental analysis.

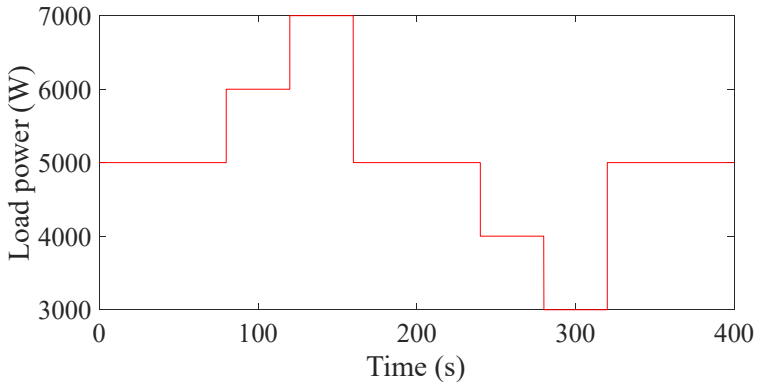

Figure 18. The load power.

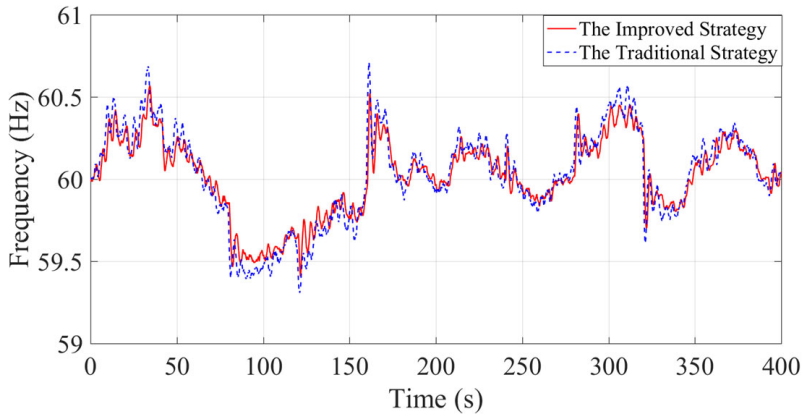

Figure 19. Frequency regulation effect.

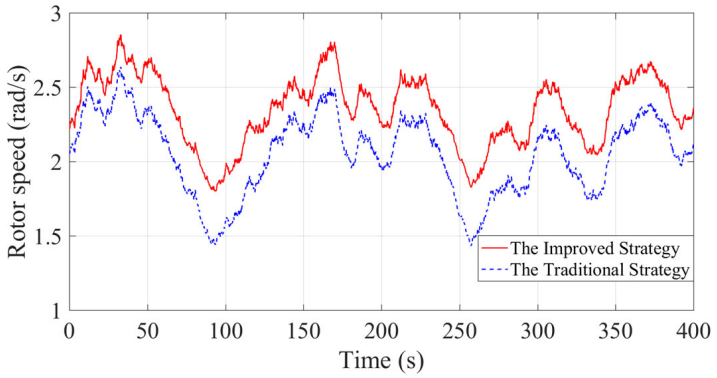

Figure 20. Rotor speed of the experiment.

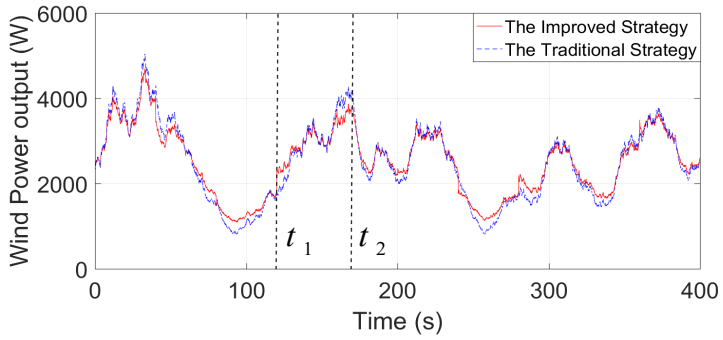

Figure 21. Wind power output of the experiment.

It can be seen from Figure 19 that the frequency fluctuation of the improved strategy in this paper is significantly smaller than that of the traditional strategy in the case of sudden load changes, and the frequency deviation of the improved strategy has increased by 8.3%.

Figure 20 shows the rotor speed of the wind turbine. Compared with the traditional strategy, the rotor speed of the improved strategy in this paper is at a higher level, and the rotor speed fluctuation is small, which can effectively mitigate the fatigue damage of the rotor and improve the stall problem caused by the low rotor speed.

The wind power output in Figure 21 shows that the power fluctuation of the improved strategy in this paper is smaller than that of the traditional strategy, which also improves the frequency stability to a certain extent. In addition, wind power can be increased or decreased faster and better in the case of sudden load changes. When the load suddenly increases at time t_1, the increased power of the improved strategy is higher than that of the traditional strategy. When the load suddenly decreases at time t_2, the output power of the improved strategy can better respond to frequency changes and be reduced faster.

6. Conclusions

This paper aims at improving the performance of OSD control under turbulent wind speed, proposing an improved OSD control strategy, which improves the effect of wind power participating in power grid frequency regulation under turbulent wind speed. The main contributions and conclusions of this paper are as follows.

1. The mechanism of poor control effect of OSD control under turbulent wind speed is revealed; the OSD control has the effect of improving the output power of wind power system, thus reducing the reserved power and weakening the frequency regulation effect.
2. The influence of deloading power coefficient on reserve capacity and frequency deviation is analyzed. It is found that there is an extreme value that minimizes the reserve capacity of the wind power system, and the extreme value will change with the turbulence characteristics of turbulent wind speed.

3. The mathematical relationship between the deloading power coefficient corresponding to the minimum reserve capacity and the turbulence characteristic index is obtained, and the reasonable range of the deloading power coefficient under different wind conditions is proposed accordingly.
4. An algorithm for optimizing deloading power coefficient based on turbulence characteristics is proposed, which can make wind turbines effectively respond to different wind conditions, provide reserve capacity stably and quickly, and improve the frequency regulation effect under turbulent wind speed.

Compared with the existing methods, the simulation and experimental results based on the experimental platform show that the improved control strategy proposed in this paper has better performance in decreasing frequency deviation, degree of frequency drop, expediting rotor speed recovery and avoiding the secondary frequency drop, and that the improvement in frequency deviation can reach 19.28%.

Author Contributions: X.Z. conceived the study and wrote the paper; B.L. analyzed the problems and designed the method and simulation examples; K.X. performed the simulation examples and help to wrote the paper; Y.Z. and S.H. analyzed the data; Q.H. help to wrote the paper. All authors have read and agreed to the published version of the manuscript.

Funding: This work was supported by National Natural Science Foundation of China (52107098).

Data Availability Statement: Not applicable.

Conflicts of Interest: The authors declare no conflict of interest.

References

1. Lu, L.; Saborío-Romano, O.; Cutululis, N.A. Frequency Control in Power Systems with Large Share of Wind Energy. *Energies* **2022**, *15*, 1922. [CrossRef]
2. Liu, H.; Wang, P.; Zhao, T.; Fan, Z.; Pan, H. A Group-Based Droop Control Strategy Considering Pitch Angle Protection to Deloaded Wind Farms. *Energies* **2022**, *15*, 2722. [CrossRef]
3. Ding, L.; Yin, S.; Wang, T.X.; Liu, J. Active Rotor Speed Protection Strategy for DFIG-based Wind Turbines with Inertia Control. *Autom. Electr. Power Syst.* **2015**, *39*, 29–34.
4. Chen, Y.; Wang, G.; Shi, Q.; Fu, L.J.; Jiang, W.T.; Huang, H. A New Coordinated Virtual Inertia Control Strategy for Wind Farms. *Autom. Electr. Power Syst.* **2015**, *39*, 27–33.
5. Yan, X.; Cui, S.; Chang, W. Primary Frequency Regulation Control Strategy of Doubly-Fed Induction Generator Considering Supercapacitor SOC Feedback Adaptive Adjustment. *Trans. China Electrotech. Soc.* **2021**, *36*, 1027–1039. [CrossRef]
6. Yan, X.; Cui, S.; Wang, D.; Wang, Y.; Li, T. Inertia and Primary Frequency Regulation Strategy of Doubly-fed Wind Turbine Based on Super-capacitor Energy Storage Control. *Autom. Electr. Power Syst.* **2020**, *44*, 111–129.
7. De Almeida, R.G.; Pecas Lopes, J.A. Participation of Doubly Fed Induction Wind Generators in System Frequency Regulation. *IEEE Trans. Power Syst.* **2007**, *22*, 944–950. [CrossRef]
8. Ghosh, S.; Kamalasadan, S.; Senroy, N.; Enslin, J. Doubly Fed Induction Generator (DFIG)-Based Wind Farm Control Framework for Primary Frequency and Inertial Response Application. *IEEE Trans. Power Syst.* **2016**, *31*, 1861–1871. [CrossRef]
9. Hu, J.X.; Xu, G.Y.; Bi, T.S.; Cui, H.B. A strategy of frequency control for deloaded wind turbine generator based on coordination between rotor speed and pitch angle. *Power Syst. Technol.* **2019**, *43*, 3656–3662. [CrossRef]
10. Boyle, J.; Littler, T.; Foley, A.M. Frequency Regulation and Operating Reserve Techniques for Variable Speed Wind Turbines. In Proceedings of the 2021 IEEE PowerTech, Madrid, Spain, 28 June–2 July 2021; pp. 1–5.
11. Wang, R.; Gao, L.; Shen, J.; Wang, Q.; Deng, Y.; Li, H. Frequency Regulation Strategy with Participation of Variable-speed Wind Turbines Power System with High Wind Power Penetration. *Autom. Electr. Power Syst.* **2019**, *43*, 101–110.
12. Cui, S.; Yan, X.; Wang, Y.; Li, R.; Li, T. A Smooth Adjustment Method for Primary Frequency of Doubly-fed Wind Generators Considering Random Fluctuation Characteristics of Source-load Power. *Proc. CSEE* **2021**, *41*, 143–154. [CrossRef]
13. Zhang, X.; Zhang, Y.; Hao, S.; Wu, L.; Wei, W. An improved maximum power point tracking method based on decreasing torque gain for large scale wind turbines at low wind sites. *Electr. Power Syst. Res.* **2019**, *176*, 105942. [CrossRef]
14. Zhang, X.; Huang, C.; Hao, S.; Chen, F.; Zhai, J. An Improved Adaptive-Torque-Gain MPPT Control for Direct-Driven PMSG Wind Turbines Considering Wind Farm Turbulences. *Energies* **2016**, *9*, 977. [CrossRef]
15. Ye, H.; Pei, W.; Qi, Z. Analytical Modeling of Inertial and Droop Responses from a Wind Farm for Short-Term Frequency Regulation in Power Systems. *IEEE Trans. Power Syst.* **2016**, *31*, 3414–3423. [CrossRef]
16. Wang, H.; Yang, J.; Chen, Z.; Ge, W.; Ma, Y.; Xing, Z.; Yang, L. Model Predictive Control of PMSG-Based Wind Turbines for Frequency Regulation in an Isolated Grid. *IEEE Trans. Ind. Appl.* **2018**, *54*, 3077–3089. [CrossRef]

17. Zhang, X.; Lin, B.; Yin, M.; Hao, S.; Zhang, C.; Zuo, T. A Novel Frequency Control Method for Smart Buildings with Wind Power System Integration Considering Turbulence Characteristics. *IEEE Trans. Ind. Appl.* **2022**, *59*, 15–25. [CrossRef]
18. Li, S.; Huang, Y.; Wang, L.; Lei, X.; Tang, H.; Deng, C. Modeling Primary Frequency Regulation Auxiliary Control System of Doubly Fed Induction Generator Based on Rotor Speed Control. *Proc. CSEE* **2017**, *37*, 7077–7086, 7422. [CrossRef]
19. Yao, Q.; Liu, J.; Hu, Y.; Meng, H. Equivalent modeling and simulation for primary regulation of wind farm with asynchronous variable-speed wind turbine. *Autom. Electr. Power Syst.* **2019**, *43*, 185–192. [CrossRef]
20. Huang, C.; Li, F.; Jin, Z. Maximum Power Point Tracking Strategy for Large-Scale Wind Generation Systems Considering Wind Turbine Dynamics. *IEEE Trans. Ind. Electron.* **2015**, *62*, 2530–2539. [CrossRef]
21. Shi, Q.; Wang, G.; Li, H. Coordinated Virtual Inertia Control Strategy of Multiple Wind Turbines in Wind Farms Considering Frequency Regulation Capability. *Power Syst. Technol.* **2019**, *43*, 4005–4017.
22. Committee, I.E. *IEC 61400-1: Wind Turbines Part 1: Design Requirements*; International Electrotechnical Commission: London, UK, 2005.
23. Wang, Y.; Meng, J.; Zhang, X.; Xu, L. Control of PMSG-Based Wind Turbines for System Inertial Response and Power Oscillation Damping. *IEEE Trans. Sustain. Energy* **2015**, *6*, 565–574. [CrossRef]
24. Yin, M.; Li, W.; Chung, C.Y.; Chen, Z.; Zou, Y. Inertia compensation scheme of WTS considering time delay for emulating large-inertia turbines. *IET Renew. Power Gener.* **2017**, *11*, 529–538. [CrossRef]